On the Integrability and Chaos of an N=2 Maxwell-Chern-Simons-Higgs Mechanical Model

L.P.G. de Assis, J.A. Helayël-Neto [1]
Centro Brasileiro de Pesquisas Físicas - CCP/CBPF - Rio de Janeiro - Brasil *and*
Grupo de Física Teórica José Leite Lopes - GFT JLL
P.O. Box 91933, 25685-970
Petrópolis Brasil
F. Haas
Centro de Ciências Exatas e Tecnológicas - UNISINOS
A.L.M.A. Nogueira
CCP/CBPF, GFT JLL *and* Laboratório de Ciências Físicas - LCFIS/CCT/UENF

Abstract

We apply different integrability analysis procedures to a reduced (spatially homogeneous) mechanical system derived from an off-shell non-minimally coupled N=2 Maxwell-Chern-Simons-Higgs model, that BPS topological vortex excitations, numerically obtained with an ansatz adopted in a special - critical coupling - parametric regime. As a counterpart of the regularity associated to the static soliton-like solution, we investigate the possibility of chaotic dynamics in the evolution of the spatially homogeneous reduced system, descendant from the full N=2 model under consideration. The originally rich content of symmetries and interactions, N=2 *susy* and non-minimal coupling, singles out the proposed model as an interesting framework for the investigation of the rôle played by (super-)symmetries and parametric domains in the triggering/control of chaotic behavior in gauge systems.

After writing down effective Lagrangian and Hamiltonian functions, and establishing the corresponding canonical Hamilton equations, we apply global integrability Noether point symmetries and Painlevé property criteria to both the general and the critical coupling regimes. In the latter, as a non-integrable character is detected by the pair of analytical criteria applied, we perform suitable numerical simulations, as we seek for chaotic patterns in the system evolution. Finally, we present some Comments on the results and perspectives for further investigations and forthcoming communications.

1 Introduction and Motivation

The dynamical properties of gauge systems define a focus of great interest, as one can realize from the remarkable effort that has recently been driven to the analysis of the stability of gauge field configurations [1]. As a cornerstone of theoretical physics, gauge theories have been intensively investigated, and the actual result is a comprehensive, but non-exhaustive, picture of such a successful theoretical framework. One (promising) aspect of such systems is the room for coherent soliton solutions, that may play a crucial rôle in the understanding of physical phenomena like, for instance, the quark confinement. On the other hand, the search for chaotic regime windows in gauge theories seems to be as much important as the former analysis, defining a counterpart approach that may lead to answers to key-problems, for instance, and again, the confinement phenomenon [1]. In the eighties, a method for investigating chaos in field theories has been developed and applied to Yang-Mills systems [2]. The main idea is to reduce the model to its mechanical limit, by considering *spatially homogeneous* field configurations. The discussion of chaotic evolution in this restricted regime is conjectured to be sufficient to ensure chaotic behavior for the full field theory [3].

[1] Email: lpgassis@cbpf.br, helayel@cbpf.br, nogue@cbpf.br

In this context, a relevant focus of attention is defined by the possibility of establishing a systematic interdependence recipe for the relation between gauge symmetries and the control of chaotic dynamics. Among gauge symmetries, one should eventually care about *supersymmetric systems*, considered either as manifestations of a fundamental symmetry or as enriched models conceived to be a tool to better describe physical situations.

Planar (2+1) Maxwell-Chern-Simons-Higgs (MCSH) theories, as candidates for an effective description of high-T_c superconductors phenomena, have recently been chosen as target models to the aim of order-to-chaos transition studies. Bambah *et al.* [4] have considered both the (proven to be) integrable minimally coupled Chern-Simons-Higgs (CSH) model and its higher momenta natural extension, namely, the minimally coupled Maxwell-Chern-Simons-Higgs system. The latter failed when submitted to an integrability criterium, the Painlevé test, leaving room for a chaotic regime that happened to be confirmed by numerical Lyapunov exponents and phase plots analysis. Quite recently, Escalona *et al.* [5] have performed a similar work upon a MCSH system endowed with both minimal *and non-minimal* couplings in the interaction sector. The non-minimal coupling stands for a Pauli-type term describing a field-strength/matter-current interaction, admitted in (2+1)-D regardless of the spin of the matter field [6]. Moreover, if quantum extension is a claim, such a non-minimal coupling should be considered from the start [7]. In the work of Ref.[5], the CSH system is argued to be still integrable, while the non-minimal MCSH exhibits "alternating windows of order and chaos", as the non-minimal coupling constant g is varied, the other parameters defining a set of constant inputs. The model they adopt is the bosonic projection of an already established N=1-*supersymmetric* system. As a matter of fact, such a bosonic Lagrangian has deserved an extension endowed with *on-shell* N=2-*susy*[8]. As far as soliton solutions are a subject of interest, the N=2 extension defines the proper framework, allowing for the self-dual regime [9, 10]. Antillón, Escalona *et al.* have found, in a previous work [11], while working upon the *same* model, a self-dual *static* non-topological vortex solution, motivating their search for *spatially homogeneous* chaotic dynamics as an interesting counterpart for their former discovery. Nevertheless, even if one assumes the validity of the conjecture relating the mechanical limit to the full theory, a problem arises if the counterpart character is claimed to be rigorous: the vortex has been found in an N=2-*susy* framework, *while the varying g procedure adopted in [5] necessarily moves the system out of the N=2-susy-bosonic projection situation.* As clearly assumed in [8], a *critical coupling*, namely, $g = -e/\kappa$, has to be verified to ensure on-shell N=2-*susy*, where e is the minimal coupling constant and κ is the Chern-Simons mass parameter. Moreover, the scalar potential is forbidden to be anything but the non-topological mass-like ϕ^2 term. So, varying g while keeping e and κ constant, and adopting $V = \lambda(\phi^2 - v^2)^2$ render their model a sector of, at most, an N=1 system.

Alternatively, another planar N=2 non-minimal MCSH model has been recently proposed [12], defining a richer spectrum that presents both non-topological *and topological* self-dual static vortex solutions [13], numerically obtained after the adoption of the critical coupling relation. Such a system exhibits *off-shell-realized N=2-susy*, and is obtained from a N=1-D=4 ansatz, after dimensional reduction and a suitable N=2-covariant superfield identification. Two important differences arise, if one settles a comparison encompassing both non-minimal MCSH models: in the N=2-off-shell case, an "additional" [2] neutral scalar field takes place; also, in the N=2-off-shell case, *no relation between the coupling constants and parameters* is required to ensure N=2-*susy* (though the vortex excitations have so far been shown to prevail in the particular $g = -e/\kappa$ regime). In other words, if the model of Ref.[12] is considered, the freely varying g strategy and a topologically non-trivial scalar potential happen to be compatible with N=2-*susy*.

Motivated by these interesting features, we carry out the analysis of the reduced - mechanical - version of the bosonic-sector Lagrangian extracted from the Ref.[13]. In the next section, we present the theory, the field equations and their spatially homogeneous counterpart, the one-dimensional effective Lagrangian and the

[2] A common, improper, terminology. The "minimum" content forbids interesting excitations, like topological vortices.

associated conjugate momenta. As we detect an additional (besides the Hamiltonian) constant of motion, a convenient reparametrization is implemented, and the corresponding Hamiltonian system is displayed, ending up with the canonical Hamilton equations. In Section 3, we move back to a (general regime) second-order formulation, upon which we start our analysis of the integrability issue, adopting two alternative analytical criteria - the Noether point symmetries approach [14] and the Painlevé test procedure [16, 17]. The former strategy leads to a set of ten coupled partial differential equations which seem to possess a closed form solution only in the minimal coupling regime, $g = 0$. In the Painlevé test context, it is shown that no set of negative integer dominant exponents can be found, as the equation for the gauge field is considered, spoiling the corresponding test algorithm for the verification of a possible strong Painlevé property associated to the system we propose. The rôle played by the gauge field equation suggests that a change in the gauge sector dynamics might render a different situation for the integrability analysis. So motivated, in Section 4 we adopt the critical coupling relation regime, arriving at *first-order* equations for the gauge degrees of freedom. We present both the associated effective Lagrangian and Hamiltonian functions, as well as the corresponding iterated second-order field equations. These results enable us to re-address the Painlevé test, which indicates that the critical coupling regime presents an even worse feature concerning the presumed strict negativeness of the dominant exponents. Revisiting the Noether point symmetries approach also gives no clues on possible integrable setups. In Section 5, an analysis of chaos is performed with physically acceptable values of the parameters; the regimes characterised by $g \neq 0$, for both non-critical and critical values of g , the model becomes more stable than whenever $g = 0$. Finally, we present our Concluding Comments and we discuss the failure of the system in obeying the strong Painlevé property, a fact that may lead to the future consideration of other integrability tests. We also try to explain why $g \neq 0$ yields a more stable behavior in spite of the inherent non-linearity brought about by a non-vanishing g.

2 Describing the Model

We start [13] with:

$$\begin{aligned}\mathcal{L}_{\rm boson} &= -\frac{1}{4}F_{\mu\nu}^2 + \frac{1}{2}\partial_\mu M\partial^\mu M + \frac{1}{2}(\nabla_\mu\phi)(\nabla^\mu\phi)^* + \\ &\quad -\frac{g}{2}(\partial_\mu M)(\partial^\mu|\phi|^2) + \frac{\kappa}{2}A_\mu\tilde{F}^\mu - U, \end{aligned} \tag{1}$$

where

$$U = \frac{e^2}{8G}\left(|\phi|^2 - v^2 + \frac{2m}{e}M + 2g|\phi|^2M\right)^2 + \frac{e^2}{2}M^2|\phi|^2 \ ,$$

and $\nabla_\mu\phi \equiv (\partial_\mu - ieA_\mu - ig\tilde{F}_\mu)\phi$. G is defined as $G \equiv 1 - g^2|\phi|^2$. The field equations for the full theory read:

$$\partial_\mu F^{\mu\rho} + m\tilde{F}^\rho = -\mathcal{J}^{\,\rho} - \frac{g}{e}\varepsilon^{\mu\nu\rho}\partial_\mu\mathcal{J}_\nu \ ,$$

where $\mathcal{J}_\mu = \frac{ie}{2}(\phi^*\nabla_\mu\phi - \phi(\nabla_\mu\phi)^*)$, and also

$$\partial_\alpha\partial^\alpha M - \frac{g}{2}\partial_\alpha\partial^\alpha|\phi|^2 + \frac{e^2(|\phi|^2 - v^2 + (2\kappa/e)M + 2gM|\phi|^2)(2\kappa/e + 2g|\phi|^2)}{4G} + e^2|\phi|^2M = 0 \qquad ,$$

$$\text{and} \quad \frac{1}{2}(\nabla_\alpha \nabla^\alpha \phi)^* - \frac{g}{2}\phi^*(\partial_\alpha \partial^\alpha M) + \frac{e^2 g^2 \phi^* \left[|\phi|^2 - v^2 + (2\kappa/e)M + 2g|\phi|^2 M\right]^2}{8G^2} + \\ + \frac{e^2 \phi^* \left[|\phi|^2 - v^2 + (2\kappa/e)M + 2g|\phi|^2 M\right](1+2gM)}{4G} + \frac{e^2 \phi^* M^2}{2} = 0 \quad .$$

Adopting the gauge choice $A_0 = 0$ and imposing the spatial homogeneity, namely, $\partial_i(\forall\ field) = 0$, the phase of the scalar field becomes a variable with vanishing time-derivative, and one can eliminate it without loss of generality. So, one ends up with a real scalar field and the following set of reduced equations of motion:

$$\frac{d}{dt}\left[G\dot{A}_1\right] = -2eg\phi\frac{d}{dt}\left[\phi A_2\right] - e^2\phi^2 A_1 - \kappa\dot{A}_2 \ , \tag{2}$$

$$\frac{d}{dt}\left[G\dot{A}_2\right] = +2eg\phi\frac{d}{dt}\left[\phi A_1\right] - e^2\phi^2 A_2 + \kappa\dot{A}_1 \ , \tag{3}$$

$$\ddot{M} = \frac{g}{2}(\dot{\phi^2}) - e^2\phi^2 M - \frac{e^2(\phi^2 - v^2 + (2\kappa/e)M + 2gM\phi^2)(2\kappa/e + 2g\phi^2)}{4G} \quad ,$$

$$\ddot{\phi} = -(eA_1 + g\dot{A}_2)^2\phi - (eA_2 - g\dot{A}_1)^2\phi + g\phi\ddot{M} - e^2\phi M^2 \\ - \frac{e^2 g^2 \phi(\phi^2 - v^2 + (2\kappa/e)M + 2gM\phi^2)^2}{4G^2} + \\ - \frac{e^2\phi(\phi^2 - v^2 + (2\kappa/e)M + 2gM\phi^2)(1+2gM)}{2G} \quad .$$

The effective Lagrangian that generates these equations of motion is:

$$L = \frac{G}{2}\left[(\dot{A}_1)^2 + (\dot{A}_2)^2\right] - \frac{Q}{2}\left(A_1\dot{A}_2 - A_2\dot{A}_1\right) - \frac{e^2\phi^2}{2}\left({A_1}^2 + {A_2}^2\right) + \\ + \frac{(\dot{M})^2}{2} - g\phi\dot{\phi}\dot{M} + \frac{(\dot{\phi})^2}{2} - \frac{e^2(\phi^2 - v^2 + (2\kappa/e)M + 2gM\phi^2)^2}{8G} - \frac{e^2\phi^2 M^2}{2} \quad ,$$

where $G \equiv 1 - g^2\phi^2$ and $Q \equiv \kappa + 2eg\phi^2$.

The canonically conjugate momenta, defined, as usually, by $p = \frac{\partial L}{\partial \dot{q}}$, have the expressions:

$$\pi_1 \equiv \frac{\partial L}{\partial \dot{A}_1} = G\dot{A}_1 + \frac{Q}{2}A_2 \ , \\ \pi_2 \equiv \frac{\partial L}{\partial \dot{A}_2} = G\dot{A}_2 - \frac{Q}{2}A_1 \ , \\ p_\phi \equiv \frac{\partial L}{\partial \dot{\phi}} = \dot{\phi} - g\phi\dot{M} \ , \\ P_M \equiv \frac{\partial L}{\partial \dot{M}} = \dot{M} - g\phi\dot{\phi} \ .$$

Before we proceed to the canonical Hamilton equations, let us notice that the quantity

$$I \equiv A_2\pi_1 - A_1\pi_2 \tag{4}$$

is a constant of motion. This can easily be checked by multiplying and combining the "gauge fields" equations according to $A_2(2) - A_1(3)$. Motivated by this fact we reparametrize the gauge sector adopting polar coordinates, instead of Cartesian ones. We have: $A_1 = Acos\zeta$, $A_2 = Asen\zeta$, and the "new" set of variables is (A, ζ, ϕ, M). The Lagrangian now reads:

$$L = \frac{G}{2}\left[(\dot{A})^2 + A^2(\dot{\zeta})^2\right] - \frac{Q}{2}\left(A^2\dot{\zeta}\right) + \frac{(\dot{M})^2}{2} - g\phi\dot{\phi}\dot{M} + \frac{(\dot{\phi})^2}{2}$$
$$-\frac{e^2\phi^2A^2}{2} - \frac{e^2(\phi^2 - v^2 + (2\kappa/e)M + 2gM\phi^2)^2}{8G} - \frac{e^2\phi^2M^2}{2} \quad , \tag{5}$$

yielding the same expressions for p_ϕ and P_M, and defining $p_A \equiv \frac{\partial L}{\partial \dot{A}} = G\dot{A}$, $p_\zeta \equiv \frac{\partial L}{\partial \dot{\zeta}} = GA^2\dot{\zeta} - \frac{Q}{2}A^2$. One can easily check that $p_\zeta = -I$, resulting $\dot{p}_\zeta = 0$. The Hamiltonian reads:

$$H_{CAN.} = \frac{1}{2G}\left[{p_A}^2 + \frac{{p_\zeta}^2}{A^2} + Qp_\zeta + {p_\phi}^2 + {P_M}^2 + 2g\phi p_\phi P_M\right] +$$
$$+\frac{1}{2G}\left[(Q/2)^2 + e^2G\phi^2\right]A^2 + \frac{e^2\phi^2M^2}{2} + \frac{e^2}{8G}\left(\phi^2 - v^2 + (2\kappa/e)M + 2g\phi^2M\right)^2 \quad .$$

The canonical Hamilton equations result:

$$\dot{A} = \frac{p_A}{G} \quad ; \quad \dot{p}_A = \frac{1}{G}\left[\frac{{p_\zeta}^2}{A^3} - \left((Q/2)^2 + e^2G\phi^2\right)A\right] ;$$

$$\dot{\zeta} = \frac{1}{G}\left[\frac{p_\zeta}{A^2} + \frac{Q}{2}\right] ; \ \dot{p}_\zeta = 0 ; \tag{6}$$

$$\dot{\phi} = \frac{1}{G}\left[p_\phi + g\phi P_M\right] ;$$

$$\dot{p}_\phi = -\frac{1}{G^2}\left\{g^2\phi\left[{p_A}^2 + \frac{{p_\zeta}^2}{A^2} + {p_\phi}^2 + {P_M}^2\right] + g\phi(\kappa g + 2e)p_\zeta + g(1 + g^2\phi^2)p_\phi P_M\right.$$
$$+(\kappa g + 2e)^2\frac{\phi A^2}{4} + e^2G^2\phi M^2 + \frac{e^2g^2\phi}{4}\left(\phi^2 - v^2 + (2\kappa/e)M + 2gM\phi^2\right)^2$$
$$\left. + \frac{e^2G\phi}{2}\left(\phi^2 - v^2 + (2\kappa/e)M + 2gM\phi^2\right)(1 + 2gM)\right\} \quad ;$$

$$\dot{M} = \frac{1}{G}\left[P_M + g\phi p_\phi\right] ;$$

$$\dot{P}_M = -\frac{1}{G}\left[e^2G\phi^2M + \frac{e^2}{4}\left(\phi^2 - v^2 + (2\kappa/e)M + 2gM\phi^2\right)\left(\frac{2\kappa}{e} + 2g\phi^2\right)\right] \quad .$$

3 Integrability Analysis: General Case

We present two Lagrangian analytical criteria to address the issue of integrability: Noether point symmetries, better suited for establishing the constants of motion, and the Painlevé test, meant to check for an overall property (the dependent variables being meromorphic for movable singularities on the complex time plane) that indicates integrability.

3.1 Noether point symmetries

An important issue regarding a Lagrangian system concerns its Noether point symmetries, linking symmetries of the action functional to conserved quantities. Here we address the question of the existence of Noether point symmetries of our system following the method shown in reference [14].

We seek for infinitesimal point transformations of the form

$$\bar{A} = A + \varepsilon\eta_A \,, \tag{7}$$
$$\bar{\zeta} = \zeta + \varepsilon\eta_\zeta \,, \tag{8}$$
$$\bar{\phi} = \phi + \varepsilon\eta_\phi \,, \tag{9}$$
$$\bar{M} = M + \varepsilon\eta_M \,, \tag{10}$$
$$\bar{t} = t + \varepsilon\tau \,, \tag{11}$$

for $\eta_A, \eta_\zeta, \eta_M, \eta_\phi$ and τ functions of the fields and the time, and ε an infinitesimal parameter. These infinitesimal transformations leave the action functional invariant up to the addition of an irrelevant numerical constant if and only if the following Noether symmetry condition [14] is satisfied,

$$\begin{aligned} \tau\frac{\partial L}{\partial t} &+ \eta_A\frac{\partial L}{\partial A} + \eta_\zeta\frac{\partial L}{\partial \zeta} + \eta_\phi\frac{\partial L}{\partial \phi} + \eta_M\frac{\partial L}{\partial M} + (\dot{\eta}_A - \dot{\tau}\dot{A})\frac{\partial L}{\partial \dot{A}} + \\ &+ (\dot{\eta}_\zeta - \dot{\tau}\dot{\zeta})\frac{\partial L}{\partial \dot{\zeta}} + (\dot{\eta}_\phi - \dot{\tau}\dot{\phi})\frac{\partial L}{\partial \dot{\phi}} + (\dot{\eta}_M - \dot{\tau}\dot{M})\frac{\partial L}{\partial \dot{M}} + \\ &+ \dot{\tau}\, L = \dot{F} \,. \end{aligned} \tag{12}$$

for F a function of the fields and the time. If such a function can be found, there is a Noether point symmetry and an associated Noether invariant I given by

$$I = \eta_A\frac{\partial L}{\partial \dot{A}} + \eta_\zeta\frac{\partial L}{\partial \dot{\zeta}} + \eta_\phi\frac{\partial L}{\partial \dot{\phi}} + \eta_M\frac{\partial L}{\partial \dot{M}} - \tau(\dot{A}\frac{\partial L}{\partial \dot{A}} + \dot{\zeta}\frac{\partial L}{\partial \dot{\zeta}} + \dot{\phi}\frac{\partial L}{\partial \dot{\phi}} + \dot{M}\frac{\partial L}{\partial \dot{M}} - L) - F \,. \tag{13}$$

In the Noether symmetry condition, the time derivatives are to be understood as total derivatives, e.g.,

$$\dot{\tau} = \frac{\partial \tau}{\partial A}\dot{A} + \frac{\partial \tau}{\partial \zeta}\dot{\zeta} + \frac{\partial \tau}{\partial \phi}\dot{\phi} + \frac{\partial \tau}{\partial M}\dot{M} + \frac{\partial \tau}{\partial t} \,. \tag{14}$$

Inserting in the symmetry condition the Lagrangian given by equation (5), we obtain that a cubic polynomial in the velocities must vanish. The coefficients of equal powers of velocities vanishing, we obtain a coupled set of linear partial differential equations determining both the symmetries and the Noether invariants. The cubic terms yields simply

$$\tau = \tau(t) \,, \tag{15}$$

that is, the transformed independent variable is a function of time only. The equations associated to quadratic terms, however, are a set of ten coupled partial differential equations which, apparently, do possess a closed form solution only in the minimal coupling case $g = 0$. Restricting the treatment to this almost trivial case, and proceeding to the first and zeroth order terms, we just found time-translation and ζ translation symmetries. These symmetries are associated, according to (13), to the energy and p_ζ conservation laws. These are almost obvious results, showing that the nonlinearity and coupling in the potential gives no much space for the existence of conservation laws of the system, even in the $g = 0$ case. This is a signature of non-integrability. However, other methods for investigating conservation laws of the system like Lie point symmetries [15] were not used.

3.2 Painlevé test

We now go back to a second-order configuration space formalism in order to settle the framework for the application of Painlevé test [16, 17]. The equations read

$$G^2\ddot{A} \;=\; 2g^2G\phi\dot{\phi}\dot{A}+\frac{C^2}{A^3}-\left(\frac{\kappa}{2}\right)^2A-e(\kappa g+e)\phi^2A\,, \tag{16}$$

where C stands for the constant p_ζ,

$$\begin{aligned} G^3\ddot{\phi} &= g^2G^2\phi\dot{\phi}^2-g^2G^2\phi\dot{A}^2-\frac{g^2C^2\phi}{A^2}-gC(\kappa\,g+2e)\phi-\frac{1}{4}(\kappa\,g+2e)^2\phi\,A^2+\\ &+ \frac{e\phi}{4}(\phi^2-v^2)\left[eg^2v^2-2(\kappa\,g+e)+g^2(2\kappa\,g-e)\phi^2+2eg^4\phi^4\right]\\ &- (\kappa\,g+e)\left[\kappa-ev^2\,g+(3eg-\kappa\,g^2)\phi^2-2eg^3\phi^4+(\kappa\,g+e)M\right]\phi\,M \end{aligned} \tag{17}$$

and

$$\begin{aligned} G^3\ddot{M} &= gG^2\dot{\phi}^2-g^3G^2\phi^2\dot{A}^2+\frac{g^3C^2\phi^2}{A^2}-\frac{g}{4}(\kappa\,g+2e)^2A^2\phi^2-g\,(\kappa\,g+e)^2M^2\phi^2+\\ &+ \frac{e}{4}(\phi^2-v^2)[-2\kappa+g\,(-4e+eg^2v^2+2\kappa\,g)\phi^2+3eg^3\phi^4]\\ &+ [-\kappa^2+(\kappa^2g^2+e\kappa\,g^3v^2-e^2-3e\kappa\,g+e^2g^2v^2)\phi^2+eg^2(2\kappa\,g-e)\phi^4+e^2g^4\phi^6]M\,. \end{aligned} \tag{18}$$

Assuming time to be a complex variable, the first step of the Painlevé test is concerned with the leading singularity behavior. One supposes the leading terms to be of the general form $A\sim a(t-t_0)^\alpha, \phi\sim b(t-t_0)^\beta, M\sim c(t-t_0)^\gamma$, where $\alpha,\beta,\gamma<0$. Such an assumption turns the last three equations into the following asymptotic ($t\to t_0$) relations:

$$g^4ab^4\alpha\,[\alpha-1+2\beta]\,\tau^{\alpha+4\beta-2} \;\sim\; 0\;;$$

$$\begin{aligned} g^6b^7\beta\,[2\beta-1]\,\tau^{7\beta-2} &\sim g^6b^5a^2\alpha^2\tau^{2\alpha+5\beta-2}+\\ -2eg^3(\kappa g+e)b^5c\tau^{5\beta+\gamma} &+ (\kappa g+e)^2bc^2\tau^{\beta+2\gamma}\;; \end{aligned}$$

$$c\gamma(\gamma-1)\tau^{4\beta+\gamma-2} \;\sim\; gb^2\beta(2\beta-1)\tau^{6\beta-2}\;,$$

where $\tau=t-t_0$.

Starting from the last equation, one gets $\gamma=2\beta$ and $c=gb^2/2$. Inserting $\gamma=2\beta$ in the second equation reduces the balancing to the first two terms, so leading to $\alpha=\beta$ and $a^2=(2\beta-1)b^2/\beta$. But the first equation shows the impossibility of having $\alpha,\beta<0$, as $\alpha+2\beta-1=0$ is required, spoiling the Painlevé test procedure.

Another possibility would be to set $\alpha=0$ in the first equation, leaving it behind as an identity. One could then drop the second term (first on right-hand side) of the second equation, and the balancing of the remaining three terms would lead to an interesting set of negative values for γ and β: $\gamma=-4$, $\beta=-1$, provided that the following relation holds:

$$(\kappa g+e)^2c^2-2(\kappa g+e)eg^3b^4c+3g^6b^6 \;=\; 0\,.$$

Still, one has to deal with a zero "dominant" exponent, which spoils the Painlevé test.

As one faces a problem with the gauge sector dynamics, the adoption of the critical coupling relation (projecting the system onto the regime that hosts the already established vortex excitations) may serve as a valuable tool of investigation. In fact, imposing $g = -e/\kappa$ leads to first-order equations for the gauge field [13].

4 Critical coupling regime

If $g = -e/\kappa$, one gets:

$$\kappa \tilde{F}_\nu \;\; = \;\; -\mathcal{J}_\nu \;\; ,$$

and the reduction to spatially homogeneous configurations yields

$$\kappa G \mathcal{E}_{ij}\, \dot{A}_j \;\; = \;\; -e^2\, A_i\, \phi^2 \;\; , \tag{19}$$

where $\mathcal{E}_{12} = +1 = -\mathcal{E}_{21}$. From this set of equations one can arrive at

$$G\frac{d}{dt}(A_1^2 + A_2^2) \;\; = \;\; 0 \;\; ,$$

and, as far as $G > 0$ (a condition inherited from the original N=2-*susy* framework), this implies that $A_1^2 + A_2^2$ is a constant of motion (thus reproducing the "pure" minimally coupled Chern-Simons-Higgs situation). Adopting polar coordinates, $A_1 = C cos\,\zeta$, $A_2 = C sen\,\zeta$ ($A_1^2 + A_2^2 = C^2$), and manipulating the set (19), one finds $\dot{\zeta} = -e^2\phi^2/\kappa G$. Following the same route chosen in the general (non-critical) case, we seek for the effective Lagrangian and Hamiltonian, settle the canonical equations of motion and, as we aim at the Painlevé test for integrability, iterate them to get second-order coupled differential equations. One can easily verify that the following Lagrangian and Hamiltonian functions

$$\begin{aligned} L \;\; = \;\; & p_\zeta \left(\dot{\zeta} + \frac{e^2\phi^2}{\kappa G}\right) + \frac{\dot{\phi}^2}{2} - \frac{e^2C^2\phi^2}{2} - \frac{e^4C^2\phi^4}{2\kappa^2 G} + \\ & \frac{\dot{M}^2}{2} - g\phi\dot{\phi}\dot{M} - \frac{e^2\big(\phi^2 - v^2 + (2\kappa/e)M + 2g\phi^2 M\big)^2}{8G} - \frac{e^2M^2\phi^2}{2} \;\; , \end{aligned}$$

$$\begin{aligned} H_{CAN.} = \frac{1}{2G}\left[\frac{{p_\zeta}^2}{A^2} + Qp_\zeta + {p_\phi}^2 + {P_M}^2 + 2g\phi p_\phi P_M\right] + \\ + \frac{1}{2G}\left[(Q/2)^2 + e^2G\phi^2\right]A^2 + \frac{e^2\phi^2M^2}{2} + \frac{e^2}{8G}\big(\phi^2 - v^2 + (2\kappa/e)M + 2g\phi^2M\big)^2 \qquad , \end{aligned}$$

where $g = -e/\kappa$, $G = 1 - (e^2/\kappa^2)\phi^2$, and $p_\zeta = -\kappa C^2/2$ [3], leads to the proper set of field equations. The iterated second-order system turns out to be

$$\begin{aligned} -G^3\ddot{\phi} = -g^2G^2\phi\dot{\phi}^2 + \frac{g^2C^2\phi}{A^2} + e^2\frac{\phi A^2}{4} \\ + \big[eg(C + egv^4/4)\big]\,\phi \; + \frac{e}{2}\left[-2eg^2v^2\right]\phi^3 + e^2g^2\left[1 + \frac{g^2v^2}{4}\right]\phi^5 - \frac{e^2g^4}{2}\phi^7 \;\; ; \end{aligned}$$

[3] In fact, such a relation between the conserved quantities p_ζ and $A^2\,(\equiv C^2)$ must be imposed to ensure first-order $\dot{\zeta} = -e^2\phi^2/\kappa G$ equation of motion.

$$G^2\ddot{M} = (g - 2g^3\phi^2 + g^5\phi^4)\dot{\phi}^2 + (g\phi - 2g^3\phi^3 + g^5\phi^5)\ddot{\phi} + 2e^2\phi^2 M$$
$$-e^2g^2\phi^4 M - \kappa^2 M - \frac{\kappa e}{2}\phi^2 - e^2g^2(1 + \frac{g^2v^2}{2})\phi^4 + \frac{e^2g^3\phi^6}{2} + \frac{\kappa e v^2}{2} \ .$$

Again, for the Painlevé test, the asymptotic relations are found: $\phi:\ \beta = 0$ or $\beta = 1/2$. If one takes the $\beta = 0$ case, one is left with two problematic outputs, as the equation for M is considered: either $\gamma = \beta = 0$, or $\beta = 0$, $b^2 = 1/g^2$, γ undetermined. So the signature of lack of strong Painlevé property remains.

5 Analysis of chaos

Since the results of the analytical approaches suggest that the system may not be integrable, we now turn to a numerical study to verify if such a non-integrability feature is presented in a chaotic form.

5.1 SALI method

The most well–known method used to detect whether a system is chaotic or not is the maximal Lyapunov Characteristic Exponent (LCE) σ_1. If $\sigma_1 > 0$ the flow is chaotic. The σ_1 is computed [18, 19] as

$$L_t = \frac{1}{t}\ \ln\frac{|\vec{w}(t)|}{|\vec{w}(0)|}\,, \text{ and taken the limit} \tag{20}$$

$$\sigma_1 = \lim_{t\to\infty} L_t\,, \tag{21}$$

where $\vec{w}(0)$, $\vec{w}(t)$ are deviation vectors and the time evolution of $\vec{w}$ is given by solving the *equations of motion* and your *variational equations*.

Since these vectors tend to acquire an exponential growth in short time intervals, many calculations of L_{T_1}, as $\vec{w}(t)$ evolves for a short time t_1, are carried out after each $\vec{w}(t)$ is normalizated. With this procedure, the mean value of L_{T_1} is computated as

$$\sigma_1 = \frac{1}{N}\sum_{i=1}^{N} L_{T_i}$$

For Hamiltoniam sytems, this computation becomes very lengthy with poor convergence, and this long procedure may point to a false chaos diagnostic.

We have chosen to adopt the method developed by Skokos, Antonopoulos, Boutis and Vrahatis, the so-called Smaller Alignment Index, SALI, for brevity[20, 21].The reason for this choice is that the SALI method is computationally faster and less unstable than the Lyapunov exponent analysis, improving the adequacy of the former for the system we investigate. The SALI is a indicator of chaos that tends to zero for chaotic orbits, while it exhibits small fluctuations around non-zero values for ordered ones. So, the SALI is defined as:

$$\text{SALI}(t) = \min\left\{\left\|\frac{\vec{w}_1(t)}{\|\vec{w}_1(t)\|} + \frac{\vec{w}_2(t)}{\|\vec{w}_2(t)\|}\right\|, \left\|\frac{\vec{w}_1(t)}{\|\vec{w}_1(t)\|} - \frac{\vec{w}_2(t)}{\|\vec{w}_2(t)\|}\right\|\right\}, \tag{22}$$

where $\vec{w}(t)_1$ and $\vec{w}(t)_2$ are the evolutions of two deviations vectors with different initial conditions, $\|\cdot\|$ is the Euclidean norm and t is the time .

The authors of SALI method showed that SALI can be approximate by use the difference of the two largest Lyapunov characteristic exponents σ_1 and σ_2.

The main advantage of the SALI in chaotic regions is that it uses two deviation vectors and exploits at every step the convergence from all previous steps. The SALI value tends to zero for chaotic flows at a rate which is a function of the difference of the two largest Lyapunov characteristic exponents σ_1, σ_2 as SALI $\propto e^{-(\sigma_1-\sigma_2)t}$. As usually done in numerical computations, we need to define a threshold so that a computed number be considered zero. In most of the cases, the selected value is $< 10^{-5}$. Like in the case of the Lyapunov exponent, it also happens that, in the SALI method, this is the we shall use to distiguish between order and chaos.

5.2 Equations of motion and requirements

The integration of the system was performed by means of a Gear algorithm, in a variable step mode, starting from the minimal step size h = 0.00001, and eventually getting reduced in order to preserve the value of the Hamiltonian and p_ζ, known to be constants of motion. Another constraint maintained along the integration was that G ($G \equiv 1 - g^2\phi^2$) should be greater than or equal to zero. The following first order equations of motion were used in the numerical integration:

$$\dot{A} = \frac{p_A}{G} \; ; \; \dot{p}_A = \frac{1}{G}\left[\frac{{p_\zeta}^2}{A^3} - \left((Q/2)^2 + e^2 G\phi^2\right) A\right] \; ;$$

$$\dot{\zeta} = \frac{1}{G}\left[\frac{p_\zeta}{A^2} + \frac{Q}{2}\right] \; ; \; \dot{p}_\zeta = 0 \; ;$$

$$\dot{\phi} = \frac{1}{G}\left[p_\phi + g\phi P_M\right] \; ;$$

$$\dot{p}_\phi = -\frac{1}{G^2}\left\{g^2\phi\left[{p_A}^2 + \frac{{p_\zeta}^2}{A^2} + {p_\phi}^2 + {P_M}^2\right] + g\phi(\kappa g + 2e)p_\zeta + g(1+g^2\phi^2)p_\phi P_M \right.$$
$$+(\kappa g + 2e)^2\frac{\phi A^2}{4} + e^2G^2\phi M^2 + \frac{e^2g^2\phi}{4}\left(\phi^2 - v^2 + (2\kappa/e)M + 2gM\phi^2\right)^2$$
$$\left. + \frac{e^2G\phi}{2}\left(\phi^2 - v^2 + (2\kappa/e)M + 2gM\phi^2\right)(1+2gM)\right\} \; ;$$

$$\dot{M} = \frac{1}{G}\left[P_M + g\phi p_\phi\right] \; ;$$

$$\dot{P}_M = -\frac{1}{G}\left[e^2G\phi^2 M + \frac{e^2}{4}\left(\phi^2 - v^2 + (2\kappa/e)M + 2gM\phi^2\right)\left(\frac{2\kappa}{e} + 2g\phi^2\right)\right] \; .$$

For the sake of simplicity, we have adopted the following notation:
$\zeta = q_1,\ A = q_2,\ \phi = q_3,\ M = q_4,\ p_\zeta = p_1, p_A = p_2,\ p_\phi = p_3,\ P_M = p_4.$

For each set of parametric inputs the numerical integration was performed and, SALI method used after transient damped. In the following reprensatative results are present of our findings.

5.3 Case with g=0

Since our model comes from a supersymmetric version of Maxwell-Chern-Simons-Higgs with non-minimal coupling, it is not clear that we shall recover similar dynamical properties as the ones observed in other studies [5, 4] when $g = 0$ and the model is reduced to the minimal coupling case. The two main properties found in these studies were the existence of chaos in the presence of Maxwell term and the final result is sensible to initial conditions. To verify these properties in our model, we have set the initial conditions in the fix point of the system and then varied q_3 from 0 to 2 with parameters set as $e = 2$, $k = 2$, $v = 2$ as mentioned above for the case $g = 0$. The initial conditions are $q_1(0) = 1$, $q_2(0) = 1$, $q_4(0) = 2$, $p_1(0) = 0$, $p_2(0) = -1$, $p_3(0) = 0$ and $p_4(0) = 0$.

The results are presented in a sequence of phase diagrams. In Figure1, we display p_4 versus q_4. We remember that we could have used any pair of variables to perturb the initial fix point and then present in these graphs, but our choice was guided by the fact both variables $q_3\,(\phi)$ and $q_4\,(M)$ are present in Higgs-type potential of our model. After this, in the Figure 2, we show a graph of SALI as function of q_3.

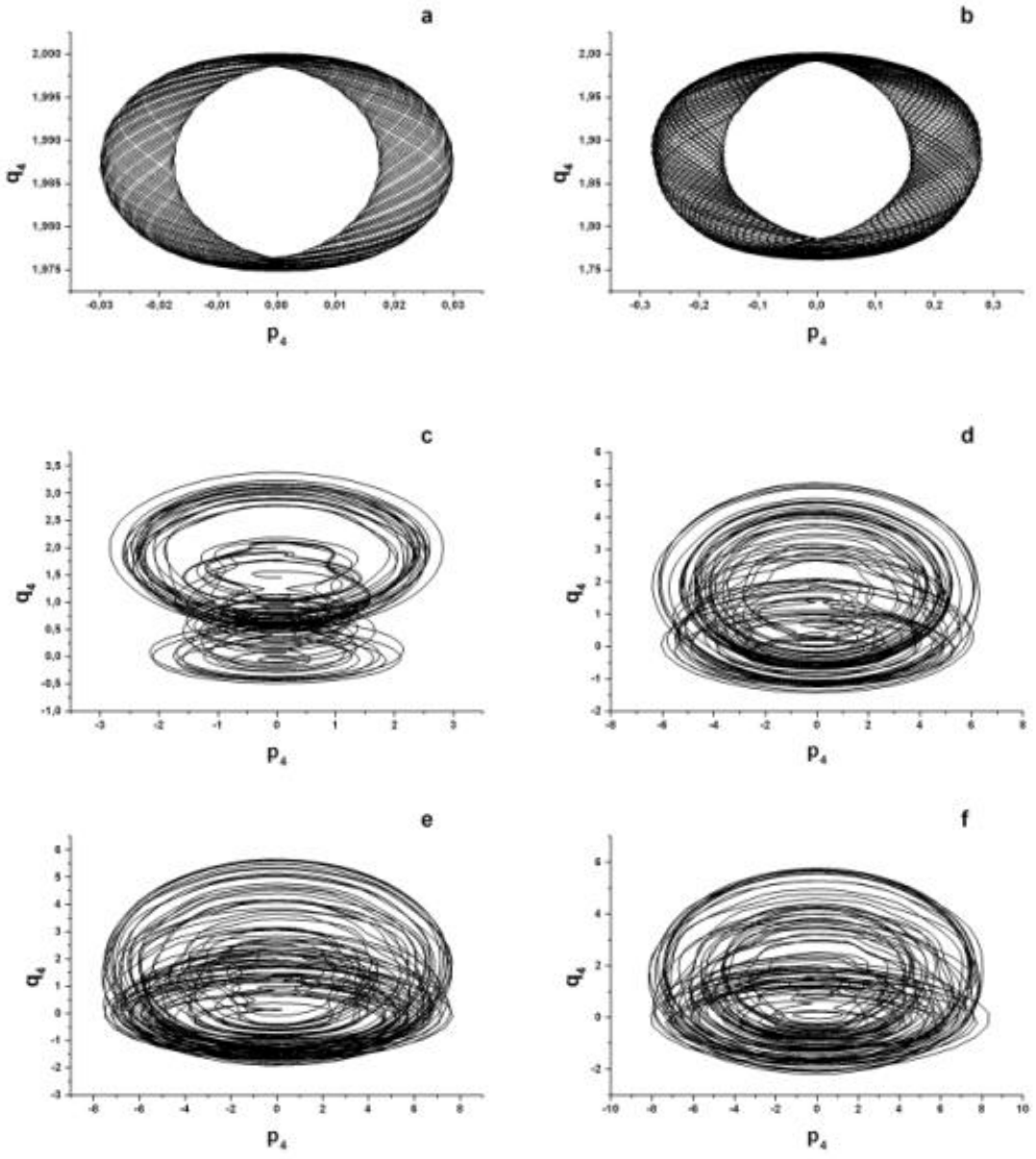

a)$q_3(0) = 0.1$, b)$q_3(0) = 0.3$, c) $q_3(0) = 0.7$, d)$q_3(0) = 1.5$, e) $q_3(0) = 1.75$ and f) $q_3(0) = 2.0$.
Figure 1

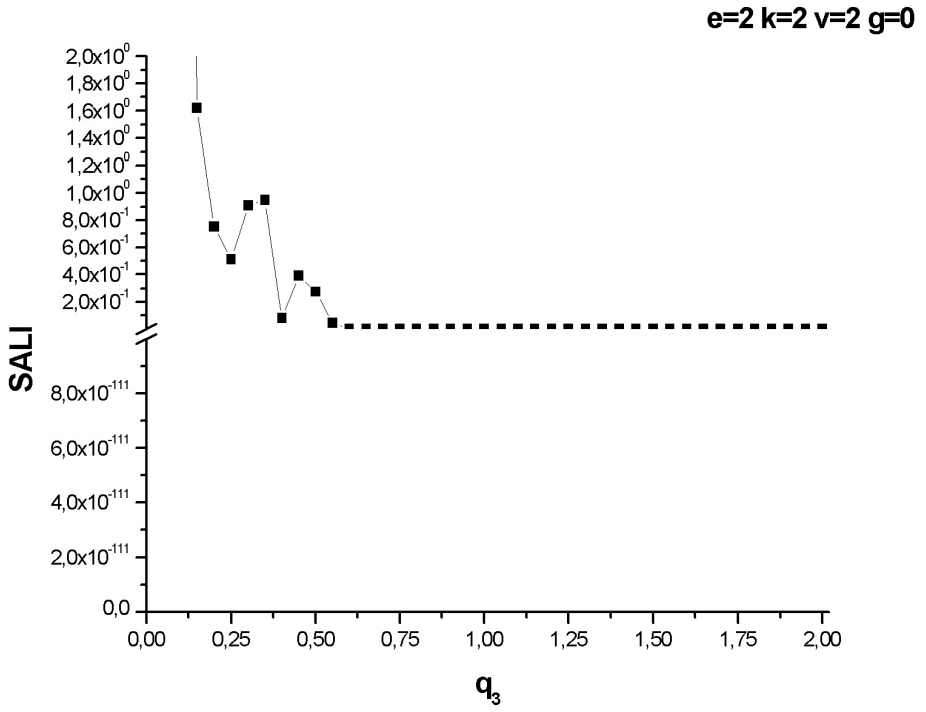

Figure 2

We can see from Figure 2, with the help of break in the vertical axes, that to $q_3 \gtrsim 0.55$ the behavior of the system becomes chaotic with SALI assuming values between 10^{-89} and 10^{-33}.

5.4 Case with g $\neq 0$ but outside critical coupling regime

Now, we used $g \neq 0$, but outside critical coupling regime, to check whether the inclusion of this kind of coupling may turn some configuration dynamics into chaotic, with initial conditions that, in the case $g = 0$, were regular. To do that, we fix the parameters and the initial conditions as $e = 2$, $k = 2$, $v = 2$ and $q_1(0) = 1$, $q_2(0) = 1$, $q_3(0) = 0.25$, $q_4(0) = 2$, $p_1(0) = 0$, $p_2(0) = -1$, $p_3(0) = 0$ and $p_4(0) = 0$ and we analyzed the model with the following values of g: 0.1, 0.7, 1.5 and 2.5.

For all these cases, the the behavior remained constant, indicating that the variation of g does not change the behavior of the system from regular to chaotic, as we can see in Figure 3.

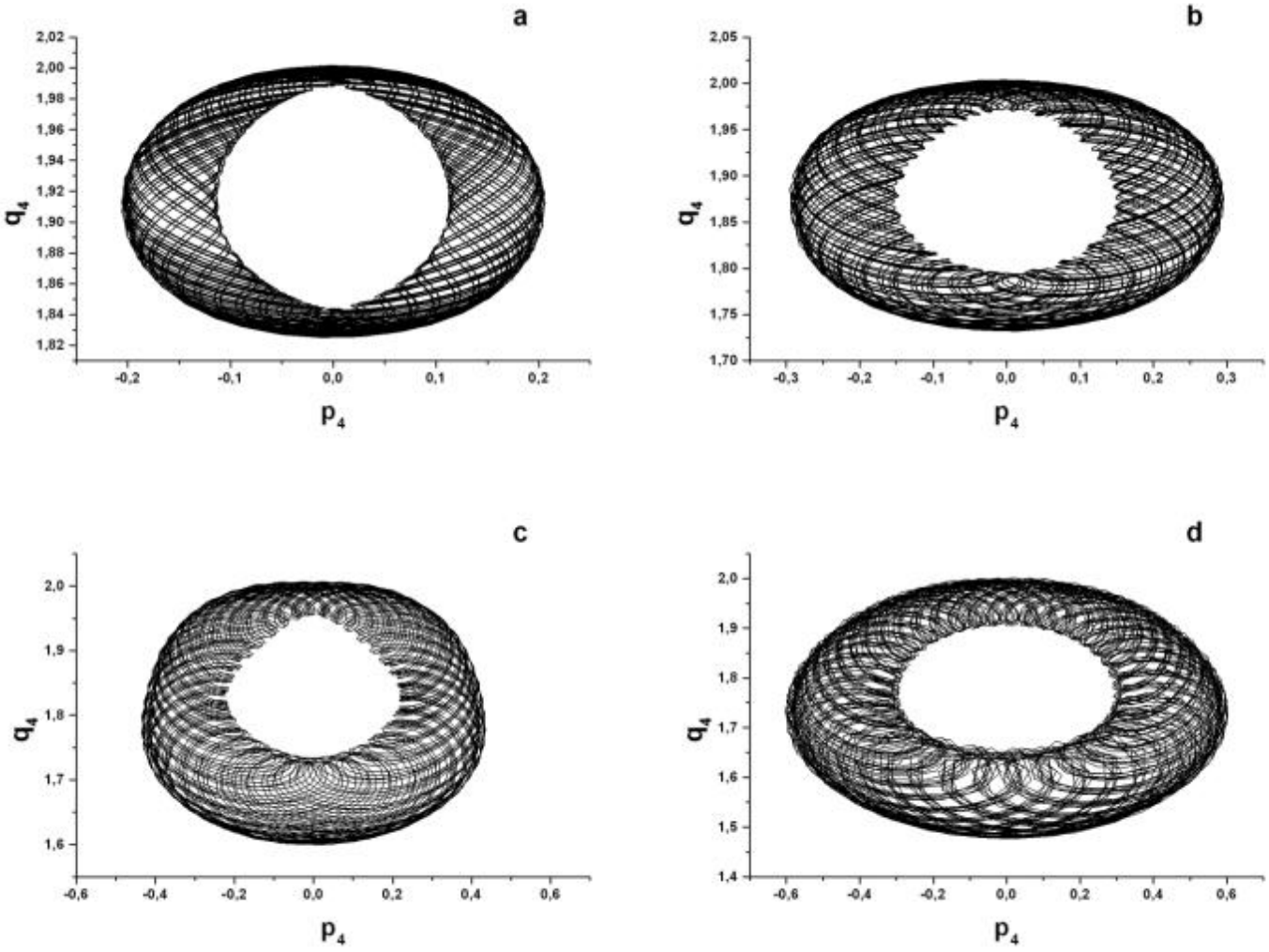

a)g=0.1,b) g=0.7,c) g=1.5 and d) g=2.5.
Figure 3

5.5 Case with g in the critical coupling regime

Now, we explore the critical coupling regime where $g = -\frac{e}{k}$. We fix the parameters $k = 2$, $v = 2$ and vary e , keeping the initial conditions as a perturbation case of the fix point; but, in this case, we shall have a different set of initial conditions for each e, since the general expression for fix point element p4(0) depends on e. With this in mind, we keep the same values for $q_1(0) = 1$, $q_2(0) = 1$, $p_1(0) = 0$, $p_2(0) = -1$, $p_3(0) = 0$, $p_4(0) = 0$ and set $q_3(0) = 0.7$ a value that makes the system chaotic in the case $g = 0$ and $q_4(0) = e$. In this case, $q_3(0) = 0.7$ is the perturbation, since in the fix point $q_3(0) = 0.0$. As in the case g=0, we plotted a

set of phase diagrams and a graph of e versus SALI. In the SALI graphs, we break the vertical axis to show that the minimal SALI values are above the thresold of chaos, according to the expectations of the SALI method, that is, SALI $< 10^{-5}$.

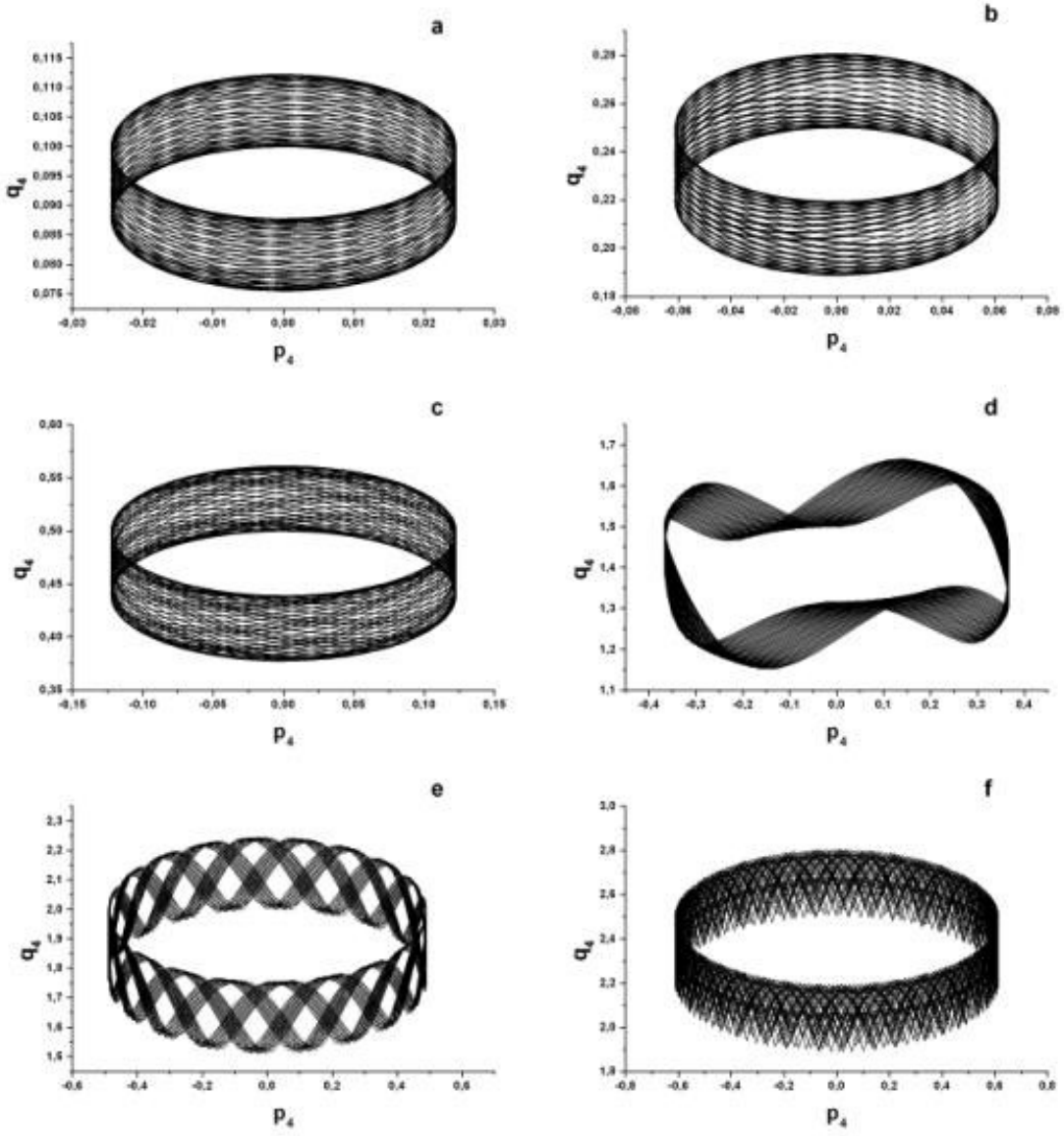

$q_3(0) = 0.7$ and e varying as a)$e = 0.10$, b)$e = 0.25$, c) $e = 0.50$, d)$e = 1.5$, e) $e = 2.0$ and f) $e = 2.5$.

Figure 4

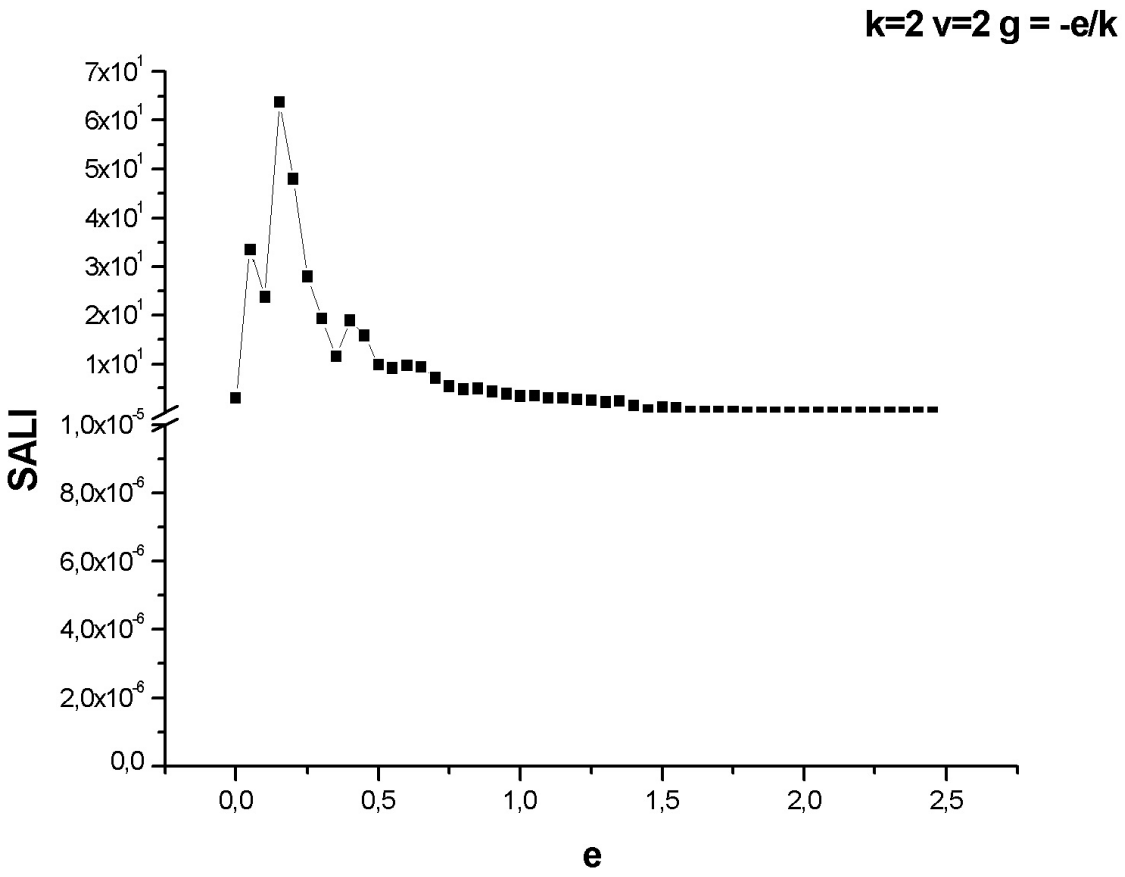

Figure 5

6 Concluding comments

The comparison between the integrable critical coupling "pure Chern-Simons" system, presented in the work of Ref.[5], and our extended N=2-*susy* descent model, the latter deserving an integrability analysis procedure both for the general and critical coupling regimes, as reported here, suggests that the extra *susy* may be responsible [22] for the global non-integrability (in the Painlevé sense) situation found even in the C.S.-like regime.

In studying chaos,two main possibilities have been checked. First, we have verified if non-vanishing values of g were able to drive the system (previously with initial conditions and parameters such that regularity was achieved for $g = 0$) into a chaotic regime. The second point we have tackled concerns the opposite effect, namely, if a chaotic configuration for $g = 0$ may become regular whenever g becomes non-trivial.

In the case of a non-critical coupling, as g increases from zero, a stable configuration for $g = 0$ keeps its stability as g varies. In those cases, the difference is that, for value s larger of g, the system becomes slightly

more unstable, but its dynamics is still regular. Something similar happens for configurations that exhibit chaos for g=0. In such cases, the system remains chaotic, but a little more unstable. For critical coupling, orbits that were chaotic for $g = 0$ become now regular; this may indicate that the critical coupling plays the rôle of a stabiliser of our model. Those results may be basically understood on the basis of two points:

1. For the critical coupling regime, there occurs a partial decoupling between the variables ϕ and M, andthis reduces the non-linearity of the system.

2. The quantity $G(G = 1 - g^2\phi^2)$ must be positive, with $0 < \phi <= 1$. This must be so in order to ensure positivity of the energy, and then existence of a stable ground state. In Eqs. (16),(17) and (18), G appears in the LHS, and for large enough g and ϕ, G becomes small, while implies a small differential variation of the system. This fact may have a stabilising consequence, implying that, in the case of a non-critical coupling, the dynamics for $g \neq 0$ is not that different from the case with $g = 0$. In the critical coupling regime, together with what we mentioned above, this may the justification of the stabilising effect.

It is also noteworthy to point out that, for negative values of G, the phase space volume is no longer conserved, and, as a consequence, we do not have any longer a Hamiltonain system. For this reason, the results reported above make sense only if the initial conditions and the parameters ensure the positivity of G. We should remind that the physical conditions imposed on the model which is supersymmetry in the origin exhibit configurations with more regular behavior than the results found in Ref.[5], as g increases.

References

[1] B.A. Bambah, C. Mukku, M.S. Sriram, S. Lakshmibala, hep-th/0203177 and references therein.

[2] S.G. Matinyan, G.K. Savvidy, N.G.T. Savvidy, Sov. Phys. JETP **53** (1981) 421.

[3] E.S. Nikolaevskii, L.S. Shur, JETP Lett. **36** (1982) 218.

[4] B.A. Bambah, S. Lakshmibala, C. Mukku, M.S. Sriram, Phys. Rev. **D47** (1993) 4677.

[5] J. Escalona, A. Antillón, M. Torres, Y. Jiang, P. Parmananda, Chaos **10** (2000) 337.

[6] J. Stern, Phys. Lett. **B265** (1991) 119.

[7] I.I. Kogan, Phys. Lett. **B262** (1991) 83.

[8] P. Navrátil, Phys. Lett. **B365** (1996) 119.

[9] E. Witten, D.I. Olive, Phys. Lett **B78** (1978) 97.

[10] E.B. Bogomol'nyi, Sov. J. Nucl. Phys. **24** (1976) 449.

[11] A. Antillón, J. Escalona, M. Torres, Phys. Rev. **D55** (1997) 6327.

[12] H.R. Christiansen, M.S.Cunha, J.A.Helayël-Neto, L.R.U. Manssur and A.L.M.A. Nogueira, Int. J. Mod. Phys. **A14** (1999) 147.

[13] H.R. Christiansen, M.S.Cunha, J.A.Helayël-Neto, L.R.U. Manssur and A.L.M.A. Nogueira, Int. J. Mod. Phys. **A14** (1999) 1721.

[14] Sarlet, W. & Cantrijn, F. *Generalizations of Noether's Theorem in Classical Mechanics.* SIAM Rev. **23** (1981) 467-494.

[15] Olver, P. J. *Applications of Lie Groups to Differential Equations.* Graduate Texts in Mathematics No. 107. Springer-Verlag: New York, 1986.

[16] M.Tabor, Chaos and Integrability in Non-Linear Dynamics : An Introduction (John Wiley & Sons, Inc., New York, 1989).

[17] M.J. Ablowitz, A. Ramani, H. Segur, Lett. Nuovo Cim. **23** (9), 333 (1978).

[18] G.Benettin, L. Galgani, A. Giorgilli, J.M. Strelcyn, Meccanica **15**, 21 (1980).

[19] A. Wolf,J.B. Swift, H.L. Swinney, J.A. Vastano, Physica D **16**, 285 (1985).

[20] Skokos, C; Antonopoulos, C; Bountis, TC; Vrahatis, MN., Detecting order and chaos in Hamiltonian systems by the SALI method, J. Phys. A-Math. Gen. 37 (240, 6269-6284 2004.

[21] Skokos, C; Antonopoulos, C; Bountis, TC; Vrahatis, MN, How does the Smaller Alignment Index (SALI) distinguish order from chaos?, Prog. Theor. Phys. Suppl. (150), 439-443. 2003.

[22] As an example of "susy-spoiling" of integrability we suggest J.M. Evans, J.O. Madsen, Phys. Lett. **B389** (1996) 665.